British Journal of Pharmacology (1995) 116, 2838-2844

Activation of nicotinic acetylcholine receptors expressed in quail fibroblasts: effects on intracellular calcium

[1]K.M.L. Cross, S.D. Jane, *A.E. Wild, R.C. Foreman & J.E. Chad

Department of Physiology & Pharmacology and *Department of Biology, University of Southampton, Southampton SO16 7PX

1 The aim of these experiments was to determine the ability of the muscle-type nicotinic acetylcholine receptor (AChR) stably expressed in quail fibroblasts (QF18 cells) to elevate intracellular calcium ($[Ca^{2+}]_i$) upon activation. Ratiometric confocal microscopy, with the calcium-sensitive fluorescent dye Indo-1 was used.

2 Application of the nicotinic agonist, suberyldicholine (SDC), to the transfected QF18 cells caused an increase in $[Ca^{2+}]_i$. Control $[Ca^{2+}]_i$ levels in QF18 cells were found to be 164 ± 22 nM (mean $\pm$ s.e.mean; $n=40$ cells) rising to 600 ± 81 nM on addition of SDC (10 μM; $n=15$ cells), whereas no increase in $[Ca^{2+}]_i$ was seen in non-transfected control QT6 fibroblasts (before: 128 ± 9 nM, $n=40$; after: 113 ± 13 nM, $n=15$).

3 The increase in $[Ca^{2+}]_i$ caused by application of SDC was dose-dependent, with an EC_{50} value of 12.7 ± 5.9 μM ($n=14$).

4 The responses to SDC in QF18 cells were blocked by prior application of α-bungarotoxin (200 nM), by the addition of Ca^{2+} (100 μM), by removal of Na^+ ions from the extracellular solution, or by the voltage-sensitive calcium channel blockers nifedipine and ω-conotoxin, which act with IC_{50} values of 100 nM and 100 pM respectively.

5 We conclude that activation of the nicotinic AChRs leads to a Na^+-dependent depolarization and hence activation of endogenous voltage-sensitive Ca^{2+} channels in the plasma membrane and an increase in $[Ca^{2+}]_i$. There is no significant entry of Ca^{2+} through the nicotinic receptor itself.

Keywords: Nicotinic acetylcholine receptors; confocal laser scanning microscopy; suberyldicholine; voltage-sensitive calcium channels; quail fibroblasts; Indo-1; nifedipine; ω-conotoxin

Introduction

In this study we have investigated the ability of muscle foetal-type nicotinic acetylcholine receptors (AChRs) to elevate intracellular calcium ion $[Ca^{2+}]_i$ levels either directly via entry of Ca^{2+} through the activated channels, or indirectly via membrane depolarization and hence activation of voltage-gated calcium channels.

Biophysical analysis of nicotinic AChR channels has shown that the muscle nicotinic AChR and the neuronal nicotinic AChRs have both Ca^{2+} and Na^+ conductance, but that the neuronal forms have greater Ca^{2+} permeability than muscle forms, indeed the α_7 homomer is thought to be 10 to 20 times more permeable to calcium than sodium ions (Bertrand *et al.*, 1993; Seguela *et al.*, 1993). Neuronal nicotinic receptors in the chick ciliary ganglion have been shown to increase intracellular calcium in two ways, by being permeable to calcium themselves, and through activation of voltage-gated calcium channels (Rathouz & Berg, 1994). However, it is not clear whether the Ca^{2+} ions entering via the foetal nicotinic AChR channel can produce a physiologically significant elevation in $[Ca^{2+}]_i$ which may be important in the formation of the neuromuscular junction (Peng, 1984; Rotzler *et al.*, 1991), or whether any elevations are secondary to membrane depolarization. It has been suggested from single channel studies (Decker & Dani, 1990), that the single channel calcium influx is significant, carrying around 2% of the total inward current through the nicotinic AChR in BC3H-1 mouse muscle cells under physiological conditions.

We have investigated Ca^{2+} signalling in a surrogate expression system, the quail fibroblast, a cell line which shares a common developmental origin with myoblastic cells (Willmer, 1970). This avoids the difficulties of studies in intact neuromuscular preparations due to the structural complexity and the numbers of possibly participating molecular elements. We have used a quail fibroblast cell line, designated QF18, which has been stably transfected with cDNAs encoding the four subunits of the foetal-type mouse muscle nicotinic AChR (Phillips *et al.*, 1991). The kinetics of the nicotinic AChR channel are affected by the expression system, and from patch clamp analysis, those expressed in QF18 cells exhibit conductance and burst properties typical of foetal-type receptors *in situ* (Mishina *et al.*, 1986; Anderson *et al.*, 1977; Covarrubias & Steinbach, 1990; Phillips *et al.*, 1991). The non-transfected parental cell line QT6 (Moscovici *et al.*, 1977), expresses no detectable endogenous nicotinic AChR (Blount & Merlie, 1988). We have used Confocal Laser Scanning Microscopy (CLSM) to develop a quantitative method of studying the changes in $[Ca^{2+}]_i$ in response to agonists and blockers and have used this system to investigate the ability of the muscle type nicotinic receptor to increase intracellular calcium. We have shown that application of nicotinic agonists to the transfected QF18 cells, but not to non-transfected QT6 cells, causes a reproducible rise in $[Ca^{2+}]_i$. The mechanism underlying this response has been further investigated by changing the composition of the extracellular solution and the use of blockers, determining that the increase is not via calcium entry through the nicotinic receptor itself, but through voltage-gated calcium channels. Preliminary data have been published in abstract form (Cross *et al.*, 1995).

Methods

In this study we have used CLSM in conjunction with the ratiometric calcium-sensitive fluorescent indicator dye Indo-1 (Phenna *et al.*, 1995), to measure the $[Ca^{2+}]_i$ levels in living

[1] Author for correspondence.

quail fibroblasts. Indo-1 is a fluorescent derivative of the calcium chelator BAPTA, the emission maxima of which changes from 485 nm in Ca^{2+}-free medium, to 405 nm when the dye is saturated with Ca^{2+} (Gryniciewicz *et al.*, 1985). The signal at each of the two emission maxima can be measured simultaneously, and the ratio of these two values used to calculate the calcium concentration according to the equation of Gryniciewicz *et al.* (1985). Indo-1 has a K_d for calcium of 251 nM (Gryniciewicz *et al.*, 1985). The use of a ratiometric dye makes the measurement of the calcium concentration independent of factors such as dye loading, cell thickness, photobleaching by the laser, and dye leakage (Diliberto *et al.*, 1994).

The cells were grown in Medium 199 (Gibco BRL) supplemented with 5% FBS, 1% dimethylsulphoxide (DMSO), 1% penicillin/streptomycin solution (10000 u/10 mg ml^{-1}) and 10% tryptose phosphate broth, and incubated at 37°C with 5% CO_2. They were plated into thin glass-bottomed wells, diameter 2 cm, for confocal imaging. Labelling of the cells with α-bungarotoxin (α-BGT) was performed by incubating them for 20 min in medium supplemented with 200 nM α-BGT, with or without the fluorescein isothiocyanate (FITC) label. The cells were then washed 3 times with normal medium and visualized. Cells were loaded with the acetoxy-methyl ester of Indo-1 by incubating them in medium supplemented with the dye at a concentration of 10 μM for 30 min under normal conditions, and then rinsed with fresh medium. Image pairs of the cells were collected at two emission wavelengths (405 nm and 485 nm; excitation wavelength 351 nm) using a modified Bio-Rad MRC-600 CLSM system. The $[Ca^{2+}]_i$ was calculated from average fluorescence ratios measured from a 140 μm^2 area within each cell. The calculation uses the experimental ratios, the signals from the dye when maximally and minimally saturated under the experimental conditions, and the calibration equation of Gryniciewicz *et al.* (1985). The maximal and minimal dye signals were determined at the end of the experiment by exposing the loaded cells to medium containing a mixture of ionophores and pump inhibitors (ionomycin 10 μM, valinomycin 6 μM, monensin 100 μM, nigericin 6 μM, and ouabain 5 mM) to obtain a saturated calcium measurement of the dye, and then adding 10 mM EGTA to obtain the minimal value.

Drugs and compounds used were suberyldicholine (SDC), ω-conotoxin GVIA, α-BGT, FITC-α-BGT, ionomycin, valinomycin, monensin, nigericin, ouabain (all Sigma, Poole, UK), and nifedipine (Calbiochem, Beeston, UK). All compounds were dissolved and added in normal complete growth medium, except for nifedipine, which had to be dissolved in a solution of 15% v/v PEG 400, 15% ethanol and 70% sterile water at 500 μM, and then diluted in complete growth medium for use. Control experiments were performed to ensure that the amount of vehicle in the final drug dilutions had no effect. Drugs were added directly to the chamber after aspirating off the medium present. In all experiments a paired design was used in which we initially tested all dishes for nicotinic response and rejected those in which less than about 30% of the cells responded to SDC (10 μM). For those experiments performed in Na^+-free solutions, a solution based on standard oocyte saline (composition (mM): NaCl 100, Ca_2Cl 1.8, KCl 2, $MgCl_2$ 1, HEPES 5, pH = 7.6) with Tris-HCl used to replace the sodium ions, was used. Again control experiments to check the viability of the cells in this medium were performed.

Results

The background $[Ca^{2+}]_i$ signal was measured in each cell type loaded with Indo-1, and then the effect of a dose of SDC (10 μM) was ascertained. Figure 1a is a phase-contrast image of the QF18 cells showing their fibroblastic morphology, and Figure 1b shows the control calcium level in the same field of cells, which was 164 ± 22 nM (mean ± s.e.mean; $n = 40$ cells). On addition of SDC (10 μM) to QF18 cells, $[Ca^{2+}]_i$ rose rapidly to a peak. Figure 1c shows the peak calcium response to 10 μM SDC, which was 600 ± 81 nM ($n = 15$ cells; $P < 0.001$). In all dishes we found that only some, 46 ± 5% ($n = 255$; 10 fields of

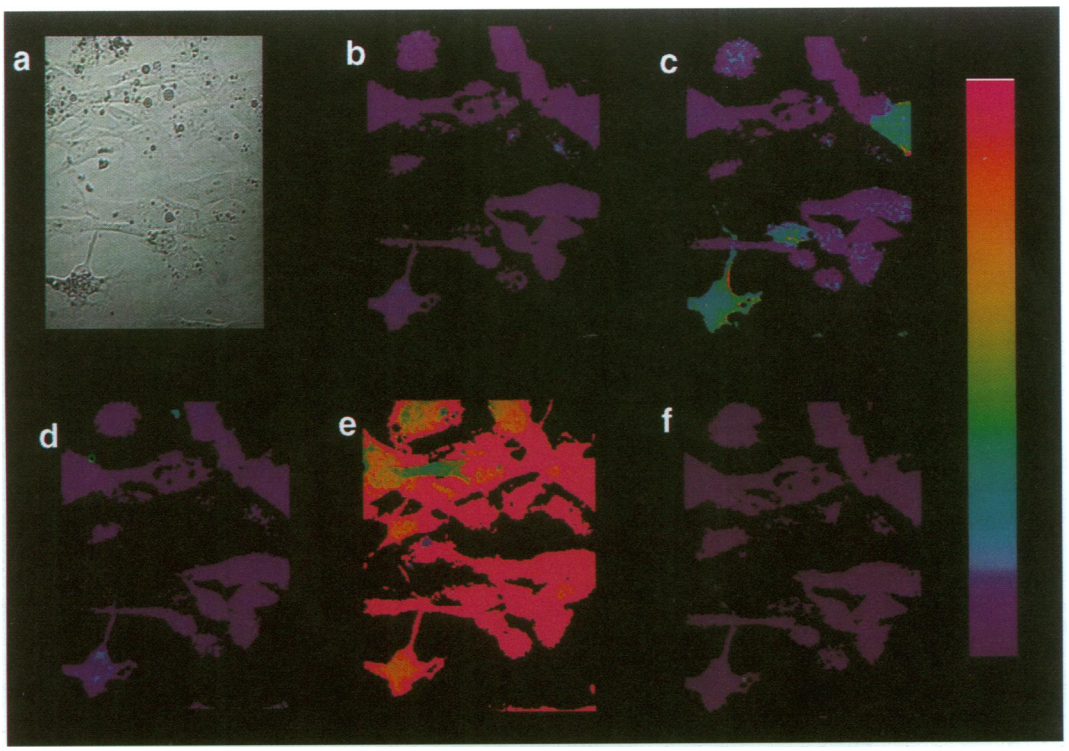

Figure 1 Suberyldicholine (SDC) causes an increase in $[Ca^{2+}]_i$ in QF18 cells. (a) Phase contrast image of the QF18 cells showing their fibroblastic morphology. (b) The control calcium signal in the same cells, which was 164 ± 22 nM ($n = 40$ cells). (c) The peak calcium signal in response to addition of SDC (10 μM) was 600 ± 81 nM ($n = 15$ cells). (d) Washing the cells returned the $[Ca^{2+}]_i$ level to control values. The intensity values have been rendered into false colour according to the colour bar, from 100 nM (purple) to greater than 1 μM (pink). (e) The cells after exposure to the ionomycin calibration solution to saturate the dye. (f) The cells after exposure to the EGTA calibration solution to obtain the minimal value for the dye.

cells), and never all, of the cells responded to the addition of agonist. Figure 1d shows that washing returns the calcium signal to control levels. In order to calibrate the calcium signal, the dye intensity ratio was measured under maximal and minimal conditions. Figures 1e and 1f show QF18 cells after exposure to ionomycin (10 μM; saturating) and EGTA (10 mM) calibration mixes respectively. The intensity values have been rendered into false colour, increasing Ca^{2+} concentration is represented through a spectrum of purple (around 100 nM), blue, green, yellow and pink (greater than 1 μM) according to the colour bar shown in the figure. The fluorescent signal seen was due entirely to the Indo-1 signal, as unloaded cells were imaged at both wavelengths measured and found to have no significant autofluorescence (data not shown).

Addition of SDC to the non-transfected QT6 cells does not cause a rise in $[Ca^{2+}]_i$. Figure 2a is a phase-contrast image showing that the QT6 cells have a similar morphology to the QF18 cells. Figure 2b shows the control $[Ca^{2+}]_i$ level, which was 128 ± 9 nM ($n = 40$ cells), and Figure 2c shows that this is unchanged by application of 10 μM SDC (113 ± 13 nM; $n = 15$ cells), or after washout of the drug (Figure 2d). The response of the cells to SDC was found to be dose-dependent. Figure 3a shows the dose-response curve, indicating that SDC acts on these cells with an EC_{50} value of 12.7 ± 5.9 μM ($n = 4$).

We also examined the time course of the calcium signal in the QF18 cells in response to 10 μM SDC (Figure 3b). Sampling at 5 s intervals through one plane of a single representative cell is shown. The response to SDC rose rapidly to a peak, which then decayed slowly over time. Line scan data showing the transcellular distribution of Ca^{2+} is shown in Figure 3c. The line scans were taken at 140 ms intervals allowing much greater time-resolution of the calcium signal. Each plot represents the Ca^{2+} level at a succession of points along a line passing through the middle of a single cell at different time intervals during a SDC response. Each point is the mean of four pixel values. Initially the level was low and uniform across the cell, but during the initial phase of the response there was an elevation at the cell edge. By 1.1 s (final plot) the elevated Ca level was again uniform across the cell, showing no standing gradient, even though the SDC response had not peaked. Further data showing the lack of standing 3-dimensional gradient in sequential z-sections, and development of responses through time can be found on the world wide web (URL http://www.neuro.soton.ac.uk/slideshow.html).

The $[Ca^{2+}]_i$ response to SDC in the QF18 cells could be blocked by a variety of treatments. Figure 4a shows that pretreatment of the cells with α-BGT (200 nM) was able to block completely the increase in $[Ca^{2+}]_i$ in response to SDC in all cells, with the control $[Ca^{2+}]_i$ level being 75 ± 9.6 nM ($n = 14$), rising to a peak of 421 ± 55 nM ($n = 14$; $P < 0.0001$) in the presence of SDC (10 μM). Pretreatment with α-BGT followed by addition of SDC (10 μM) gave a mean $[Ca^{2+}]_i$ level of 49 ± 5.1 nM ($n = 14$). This indicates that the rise in $[Ca^{2+}]_i$ caused by addition of SDC involved activation of nicotinic AChRs. In order to determine the source of the calcium increase, Cd^{2+} (100 μM) was added to the bath. This concentration of Cd^{2+} blocks transmembrane flux either through voltage-dependent calcium channels (Hagiwara & Byerly, 1981), or other pathways (Thorn, 1995). Figure 4b shows the effect of adding Cd^{2+} (100 μM) on the SDC response in a single cell. In QF18 cells, Cd^{2+} (100 μM) completely blocked the SDC response, with the control $[Ca^{2+}]_i$ level being 200 ± 32 nM ($n = 4$), 654 ± 122 nM ($n = 7$) after application of SDC (10 μM), and 165 ± 35 nM after application of SDC (10 μM) in the presence of Cd^{2+} (100 μM; $n = 7$). The removal of sodium ions from the bathing solution (Tris substitution) also prevented the increase in $[Ca^{2+}]_i$. Removal of Na^+ reverses the sodium gradient across the plasma membrane preventing depolarization of the membrane on activation of the nicotinic AChR. Figure 4c shows that Na^+ removal prevented any change in $[Ca^{2+}]_i$ in response to SDC. The control $[Ca^{2+}]_i$ level was 146 nM ($n = 8$), and the peak $[Ca^{2+}]_i$ in response to SDC (10 μM) was 790 ± 60 nM ($n = 8$; $P < 0.001$). In the absence of Na^+ the $[Ca^{2+}]_i$ level after application of SDC (10 μM) was 133 ± 19 nM ($n = 8$). This observation provides further evidence that activation of the nicotinic AChRS leads to a Na^+-dependent depolarization and hence activation of endogenous voltage-sensitive Ca^{2+} channels in the plasma membrane.

To investigate the nature of the voltage-dependent Ca^{2+}

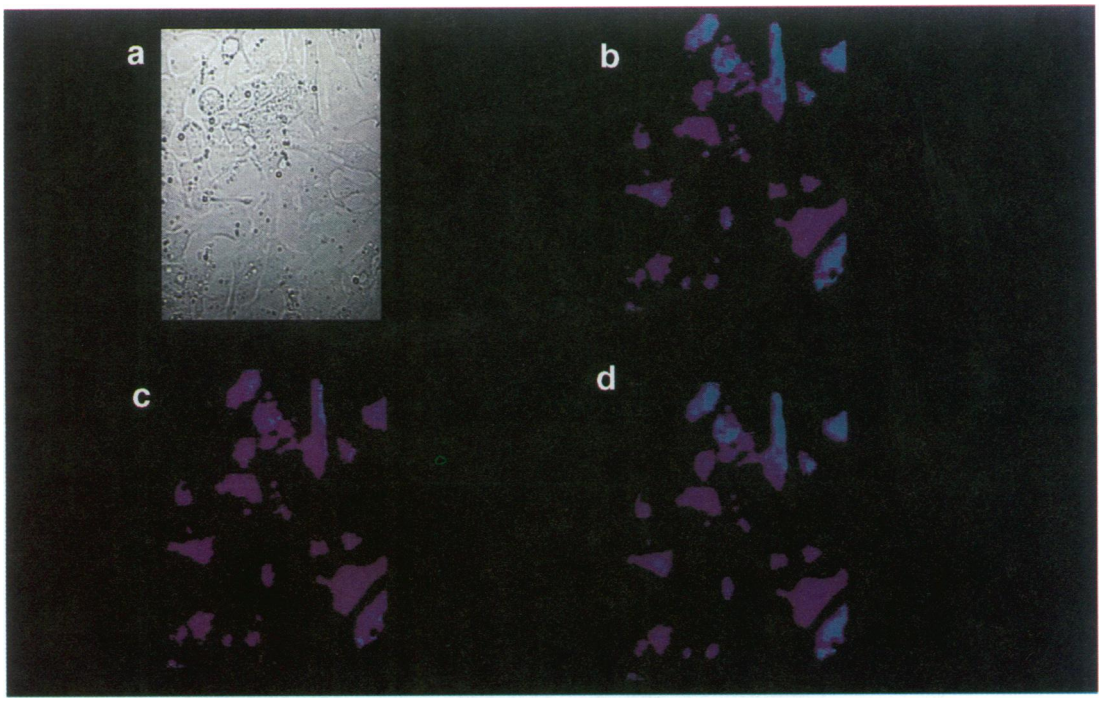

Figure 2 Suberyldicholine (SDC) does not give rise to an increase in $[Ca^{2+}]_i$ in QT6 cells. (a) Phase contrast image of the QT6 cells showing their fibroblastic morphology. (b) The control calcium signal in the same cells, which was 128 ± 9 nM ($n = 40$ cells). (c) Addition of SDC (10 μM) did not change the intracellular calcium level (113 ± 13 nM, $n = 15$ cells). (d) Washing the cells also did not alter the $[Ca^{2+}]_i$ level.

channel involved, the effects of blocking agents on the SDC response in QF18 cells were examined. Nifedipine, which blocks the L-type calcium channel (Nowycky *et al.*, 1985), and ω-conotoxin which acts at N-type calcium channels (Cruz &

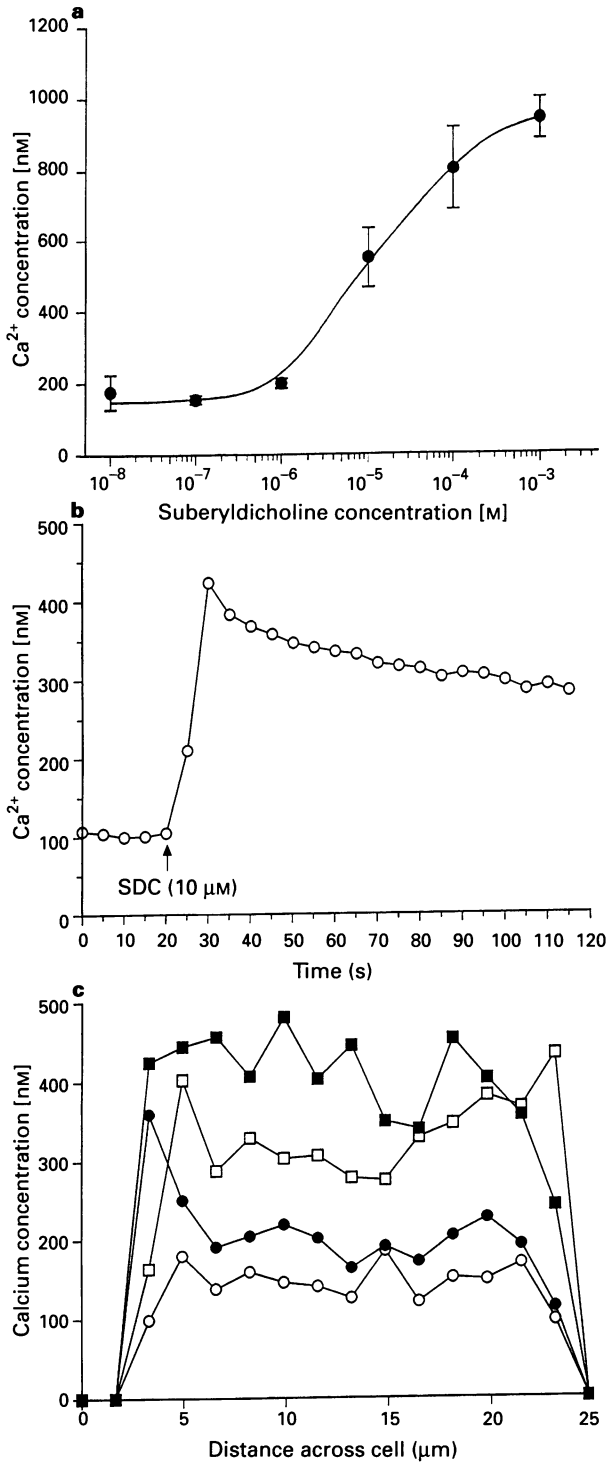

Figure 3 (a) Suberyldicholine caused an increase in $[Ca^{2+}]_i$ in QF18 cells in a dose-dependent manner. The EC_{50} value was $12.7 \pm 5.9\,\mu M$ ($n=4$). (b) The time course of the $[Ca^{2+}]_i$ signal in response to suberyldicholine (SDC) (10 μM) in a single cell. After addition of SDC, the $[Ca^{2+}]_i$ rises rapidly to a peak, which then decays slowly over time. (c) Line scan data showing the transcellular distribution of Ca^{2+}. Line scans were taken at 140 ms intervals. Each plot represents the Ca^{2+} level at a succession of points (each point is the mean of four pixel values) along a line passing through the middle of a single cell at different time intervals during a SDC response. Initially the level was low and uniform across the cell (○), but during the initial phase of the response there was an elevation at the cell edge (● = 280 ms, □ = 840 ms). By 1.1 s (■) the SDC response had not peaked, but the elevated Ca^{2+} level was again uniform across the cell, showing no standing gradient.

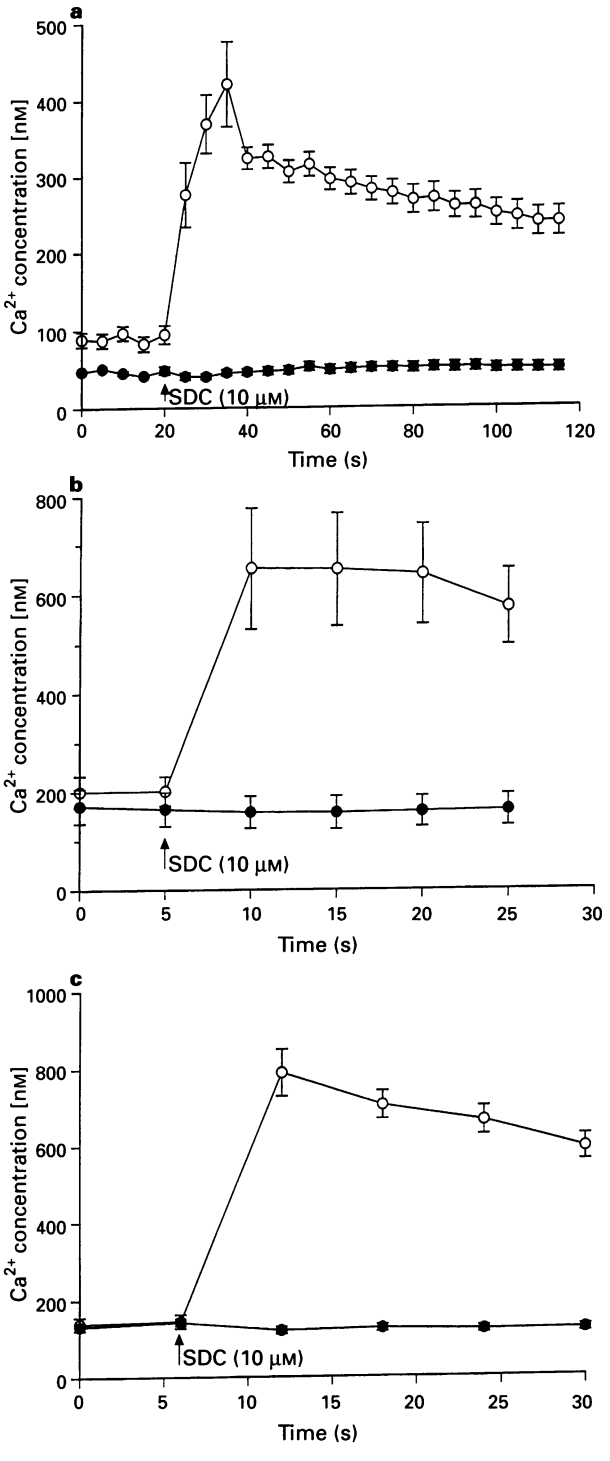

Figure 4 The response to suberyldicholine (SDC; 10 μM) can be blocked by a variety of treatments. (a) Addition of SDC (10 μM) to QF18 cells caused a rapid increase in $[Ca^{2+}]_i$ which slowly decreased with time (○). The peak response was 421 ± 55 nM ($n=14$). This response could be completely blocked by pretreatment of the cells with α-BGT (●), the calcium level was 49 ± 5.1 nM ($n=14$). (b) Graph showing data for the effect of Cd^{2+} ions (100 μM). Addition of SDC (10 μM) caused an increase in $[Ca^{2+}]_i$ from 201 ± 32 nM, to a peak value of 654 ± 122 nM ($n=7$; ●), which was blocked in the presence of Cd^{2+} (100 μM) in the extracellular medium (○); the control $[Ca^{2+}]_i$ level being 171 ± 36 nM, and 165 ± 35 nM after addition of SDC ($n=7$). (c) Application of SDC (10 μM) gave rise to a peak $[Ca^{2+}]_i$ of 790 ± 60.1 nM ($n=8$; ○), which was abolished by removal of Na^+ from the extracellular solution (●), the $[Ca^{2+}]_i$ being 133 ± 19 nM ($n=8$).

Olivera, 1986; Tsien *et al.*, 1991) were studied. We found that both compounds blocked the $[Ca^{2+}]_i$ signal in a dose-dependent manner. Figure 5a shows the dose-response curve for nifedipine. The block is expressed as the amount of inhibition by a given dose of nifedipine, with zero being no block of the $[Ca^{2+}]_i$ signal, and 1 being complete block. This was calculated by comparing the changes in $[Ca^{2+}]_i$ elicited by SDC (10 μM) with and without nifedipine. The IC_{50} for nifedipine was around 100 nM. ω-Conotoxin also inhibited the SDC response, and Figure 5b shows the dose-dependence of the ω-conotoxin effect. The strange shape of the ω-conotoxin curve, which plateaus and then rises rapidly again at concentrations above 100 nM, is probably due to the lack of specificity of the drug; at higher concentrations it will begin to block other types of Ca^{2+} channel, including the L-type. Thus the drug had an apparent high affinity IC_{50} value of around 100 pM.

Discussion

In this study we have demonstrated, by use of the ratiometric Ca^{2+}-sensitive dye Indo-1, that application of the nicotinic agonist SDC to transfected QF18, but not to non-transfected QT6 cells, causes a rapid increase in intracellular calcium concentration, which then decays slowly over time in the continued presence of the agonist. The action of SDC is dose-dependent, and in this system we have determined the EC_{50} to be 12.7 ± 5.9 μM. This value is comparable to the binding affinity and EC_{50} of SDC for nicotinic receptors at the frog endplate, which are 10 and 2.2 μM respectively (Marshall *et al.*, 1991). The response can be blocked by prior application of α-bungarotoxin (200 nM) which specifically binds to the ACh-binding site of the receptor with a half-life of dissociation of many days (Changeux, 1970). The rise in $[Ca^{2+}]_i$ in QF18 cells is thus due to activation of nicotinic receptors.

We found that in any field of QF18 cells, not all of the cells showed an increase in $[Ca^{2+}]_i$ in response to addition of SDC, probably due to lack of functional receptor protein at the cell surface. The cells were originally selected by geneticin resistance and ability to bind α-bungarotoxin (Phillips *et al.*, 1991), and without such selection pressure, in time they may revert to wild type free of receptor; the cells were transfected with a mixture of five constructs, one encoding each of the four subunits, and a fifth conferring the antibiotic resistance (Phillips *et al.*, 1991). Over time the cells may lose one or more of the subunits such that functional receptors are lost. Also, we did not incubate the cells with geneticin in the medium because in the continued presence of the antibiotic, expression of the receptor is lost altogether after about two months. In addition, the amount of protein expressed may be dependent on where the cell is in its cell cycle, or indeed, the expression of the endogenous voltage-sensitive calcium channels may change. Estacion & Mordan (1993) have demonstrated in C3H 10T1/2 mouse fibroblasts that the expression of calcium channels changes with cell density, with the fraction of cells expressing calcium channels increasing as the cell density increases.

The nature of the detected calcium signal was then investigated further. We found that it was prevented by addition of Cd^{2+} (100 μM) or removal of extracellular Na^+ ions. This data implies a transmembrane Ca^{2+} flux through voltage-gated calcium channels, which is further supported by our data on the transcellular distribution of Ca^{2+}; the U-shape of the calcium signal across the cell at very early time points indicates that the initial rise in $[Ca^{2+}]_i$ is due to entry of calcium across the membrane which then spreads through the cell.

The types of voltage-gated calcium channels involved were investigated with the Ca^{2+} channel blockers nifedipine and ω-conotoxin, which block L- and N-type channels respectively (Nowycky *et al.*, 1985; Cruz & Olivera, 1986; Tsien *et al.*, 1991). We found that both of these compounds could block the increase in $[Ca^{2+}]_i$ to some degree. These observations lead us to postulate that activation of the nicotinic AChRs by the nicotinic agonist results in a Na^+-dependent depolarization, and hence activation of endogenous voltage-sensitive L- and N-type Ca^{2+} channels in the plasma membrane. Thus we are of the opinion that these cells have at least two types of endogenous voltage-sensitive calcium channels. Fibroblasts from other species have been shown to have L- and T- calcium channel type activity (Chen *et al.*, 1988; Peres, 1989; Baumgarten, 1992; Estacion & Mordan, 1993).

As the increase in $[Ca^{2+}]_i$ observed appears to be due to entry through voltage-sensitive calcium channels, the dose-dependency of the $[Ca^{2+}]_i$ signal in response to SDC does not relate simply to occupancy of the receptors. The entry of Ca^{2+} through the Ca^{2+} channels depolarizes the cell further and stimulates the opening of yet more voltage-sensitive channels, thus this positive feedback process enhances the $[Ca^{2+}]_i$ signal at higher agonist concentrations. In addition, the $[Ca^{2+}]_i$ increase can be blocked almost completely by nifedipine, and approximately 60% by ω-conotoxin. This apparent anomaly can be explained in terms of the feedback process described above; blocking one type of voltage-sensitive calcium channel reduces overall depolarization of the cell and consequently there is less subsequent activation of other calcium channels. Each inhibitor therefore exerts a disproportionately greater

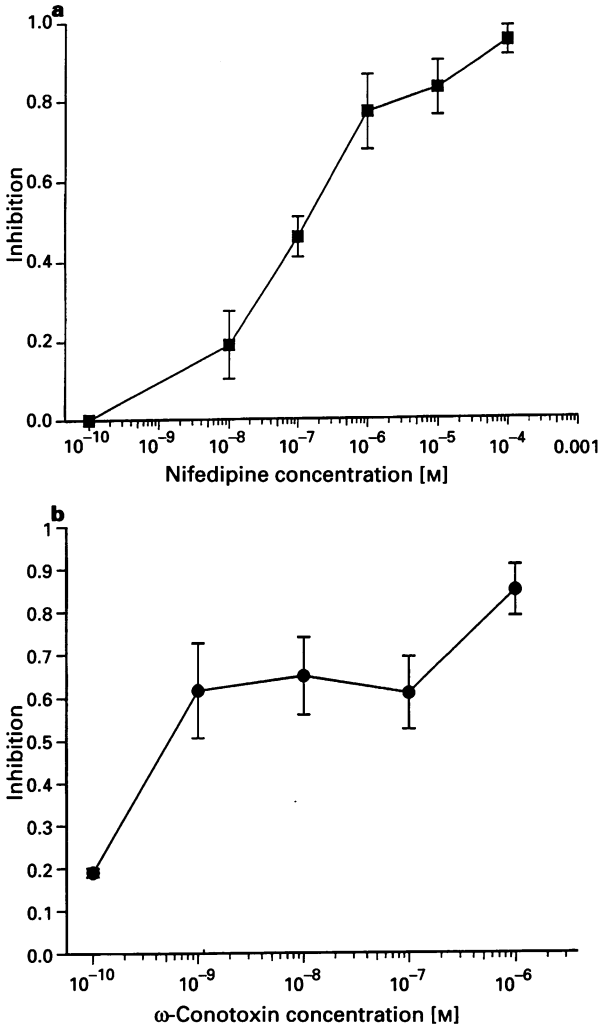

Figure 5 The increase in $[Ca^{2+}]_i$ in response to suberyldicholine (SDC) could be blocked by the voltage-sensitive calcium channel blockers, nifedipine and ω-conotoxin. (a) The dose-response curve for the effect of the L-type channel blocker nifedipine on the increase in $[Ca^{2+}]_i$ in response to SDC (10 μM). The block is expressed as the degree of block of a given dose of nifedipine, zero being no block, and 1 indicating complete block. Nifedipine acts with an IC_{50} value of 100 nM. (b) ω-Conotoxin also blocks the response to SDC (10 μM) in a dose-dependent manner, acting with an IC_{50} of around 100 pM.

effect on the observed calcium flux upon activation of nicotinic receptors. In addition, at higher concentrations it is possible that nifedipine may be blocking the nicotinic receptor itself. López *et al.* (1993) have shown that nifedipine, in the micromolar range, can block the neuronal nicotinic receptor of the bovine chromaffin cell. These receptors do not have the same pharmacology as the receptors used in our experiments; however, at high doses of nifedipine the dose-response curve appears to show a non-selectivity which may reflect some small component of direct action on the nicotinic AChR receptor.

Biophysical analysis of the conductance properties of the muscle nicotinic AChR at the single channel level in BC3H-I mouse muscle cells have shown it has some Ca^{2+} conductance (Decker & Dani, 1990); their ion-permeation model predicts that calcium contributes about 2% of the inward current in these cells under physiological conditions. However, in our study there was no measureable increase in $[Ca^{2+}]_i$ which could be attributed to the action of the nicotinic AChR channels alone. The K_d of Indo-1, which is 251 nM, (Gryniciewicz *et al.*, 1985) is comparable to the affinities of the calcium binding proteins which act as transducers of the $[Ca^{2+}]_i$ signal (for example, calmodulin has four Ca^{2+} binding sites with dissociation constants between 4 and 8 μM; Cheung, 1980) implying that the small elevations of $[Ca^{2+}]_i$ which presumably do occur in response to muscle nicotinic AChR activation are inadequate to generate a physiologically significant signal in this system.

In conclusion, we have shown functional activation of exogenous nicotinic AChRs expressed in a quail fibroblast cultured cell line, and that, whilst passage of Ca^{2+} ions through the receptor is not sufficient to produce a physiologically significant increase in $[Ca^{2+}]_i$, activation of this receptor can substantially increase $[Ca^{2+}]_i$ by subsequent activation of voltage-gated calcium channels. The ability of foetal muscle nicotinic receptors to increase intracellular calcium, by activation of voltage-gated calcium channels, may have important roles during embryonic development, in clustering (Bloch, 1983; Peng, 1984; Bloch & Steinbach, 1981) and in metabolic stabilization of nicotinic receptors (Rotzler *et al.*, 1991). We have also demonstrated the presence of at least two types of endogenous voltage-gated Ca^{2+} channels in these fibroblasts.

We would like to thank Prof J-H Steinbach for providing the QF18 and QT6 cell lines, and the Biosciences Imaging Group at the University of Southampton for the use of the Ca^{2+} imaging confocal microscope and computational data analysis facility supported by BBSRC. K.M.L.C. is a Wellcome Prize Student.

References

ANDERSON, M.J., COHEN, M.W. & ZORYCHTA, E. (1977). Effects of innervation on the distribution of acetylcholine receptors on cultured muscle cells. *J. Physiol.*, **268,** 731–756.

BAUMGARTEN, L.B., TOSCAS, K. & VILLEREAL, M.L. (1992). Dihydropyridine-sensitive L-type Ca^{2+} channels in human foreskin fibroblast cells - characterization of activation with the growth-factor Lys-bradykinin. *J. Biol. Chem.*, **267,** 10524–10530.

BERTRAND, D., GALZI, J.L., DEVILLERS-THIERY, A., BERTRAND, S. & CHANGEUX, J-P. (1993). Mutations at two distinct sites within the channel domain M2 alter calcium permeability of neuronal α7 nicotinic receptor. *Proc. Natl. Acad. Sci. U.S.A.*, **90,** 6971–6975.

BLOCH, R.J. (1983). Acetylcholine receptor clustering in rat myotubes: requirement for Ca^{2+} and effects of drugs which depolymerise microtubules. *J. Neurosci.*, **3,** 2670–2680.

BLOCH, R.J. & STEINBACH, J-H. (1981). Reversible loss of acetylcholine receptor clusters at the developing rat neuromuscular junction. *Dev. Biol.*, **81,** 386–391.

BLOUNT, P. & MERLIE, J.P. (1988). Native folding of an acetylcholine receptor α-subunit expressed in the absence of other subunits. *J. Biol. Chem.*, **263,** 1072–1080.

CHANGEUX, J-P. (1970). Use of a snake venom toxin to characterize the cholinergic receptor protein. *Proc. Natl. Acad. Sci. U.S.A.*, **67,** 1241–1247.

CHEN, C., CORBLEY, M.J., ROBERTS, T.M. & HESS, P. (1988). Voltage-sensitive calcium channels in normal and transformed 3T3 fibroblasts. *Science*, **239,** 1024–1026.

CHEUNG, W.L. (1980). Calmodulin plays a pivotal role in cellular regulation. *Science*, **207,** 19–27.

COVARRUBIAS, M. & STEINBACH, J-H. (1990). Excision of membrane patches reduces the mean open time of nicotinic acetylcholine receptors. *Pflügers Arch.*, **416,** 385–392.

CROSS, K.M.L., JANE, S.D., WILD, A.E., FOREMAN, R.C. & CHAD, J.E. (1995). Confocal imaging of calcium ion activity in quail fibroblast cultures expressing nicotinic acetylcholine receptors. *Br. J. Pharmacol.*, **114,** 441P.

CRUZ, L.J. & OLIVERA, B.M. (1986). Calcium channel antagonists: ω-conotoxin defines a new high affinity site. *J. Biol. Chem.*, **261,** 6230–6233.

DECKER, E.R. & DANI, J.A. (1990). Calcium permeability of the nicotinic acetylcholine receptor: the single-channel influx is significant. *J. Neurosci.*, **10,** 3413–3420.

DILIBERTO, P.A., WANG, X.F. & HERMAN, B. (1994). Confocal imaging of Ca^{2+} in cells. *Methods Cell Biol.*, **40,** 243–262.

ESTACION, M. & MORDAN, L.J. (1993). Expression of voltage-gated calcium channels correlates with PDGF-stimulated calcium influx and depends upon cell density in C3H 10T1/2 mouse fibroblasts. *Cell Calcium*, **14,** 161–171.

GRYNICIEWICZ, G., POENIE, M. & TSIEN, R.Y. (1985). A new generation of Ca^{2+} indicators with greatly improved fluorescence properties. *J. Biol. Chem.*, **260,** 3440–3450.

HAGIWARA, S. & BYERLY, L. (1981). Calcium channel. *Annu. Rev. Neurosci.*, **4,** 69–125.

LÓPEZ, M.G., FONTERÍZ, R.I., GANDÍA, L., DE LA FUENTE, M., VILLARROYA, M., GARCÍA-SANCHO, J. & GARCÍA, A.G. (1993). The nicotinic acetylcholine receptor of the bovine chromaffin cell, a new target for dihydropyridines. *Eur. J. Pharmacol.*, **247,** 199–207.

MARSHALL, C.G., OGDEN, D. & COLQUHOUN, D. (1991). Activation of ion channels in the frog endplate by several analogues of acetylcholine. *J. Physiol.*, **433,** 73–93.

MISHINA, M., TAKAI, T., IMOTO, K., NODA, M., TAKAHASHI, T., NUMA, S., METHFESSEL, C. & SAKMANN, B. (1986). Molecular distinctions between fetal and adult forms of muscle acetylcholine receptor. *Nature*, **321,** 406–411.

MOSCOVICI, C., MOSCOVICI, M.G. & JIMENEZ, H. (1977). Continous tissue culture cell lines derived from chemically induced tumours of japanese quail. *Cell*, **11,** 95–103.

NOWYCKY, M.C., FOX, A.P. & TSIEN, R.W. (1985). Three types of neuronal calcium channel with different calcium agonist sensitivity. *Nature*, **316,** 440–443.

PENG, H.B. (1984). Participation of calcium and calmodulin in the formation of acetylcholine receptor clusters. *J. Cell Biol.*, **98,** 550–570.

PERES, A. (1989). T-type calcium channels in swiss 3T3 fibroblasts. *Annals New York Acad. Sci.*, **560,** 116–117.

PHENNA, S., JANE, S.D. & CHAD, J.E. (1995). Increased perinuclear calcium activity evoked by metabotropic glutamate receptor activation in rat hippocampal neurones. *J. Physiol.*, **486** (1), 149–161.

PHILLIPS, W.D., KOPTA, C., BLOUNT, P., GARDNER, P.D., STEINBACH, J-H. & MERLIE, J.P. (1991). ACh receptor-rich domains organized in fibroblasts by recombinant 43-kilodalton protein. *Science (Wash DC)*, **251,** 568–570.

RATHOUZ, M.M. & BERG, D.K. (1994). Synaptic-type acetylcholine receptors raise intracellular calcium levels in neurons by two mechanisms. *J. Neurosci.*, **14,** 6935–6945.

ROTZLER, S., SCHRAMEK, H. & BRENNER, H.R. (1991). Metabolic stabilization of end-plate acetylcholine receptors regulated by calcium influx associated with muscle activity. *Nature*, **349,** 337–339.

SEGUELA, P., WADICHE, J., DINELEY-MILLER, K., DANI, J.A. & PATRICK, J.W. (1993). Molecular cloning, functional properties, and distribution of rat brain α7: a nicotinic cation channel highly permeable to calcium. *J. Neurosci.*, **13,** 596–604.

THORN, P. (1995). Ca^{2+} influx during agonist and Ins(2,4,5)P_3-evoked Ca^{2+} oscillations in HeLa epithelial cells. *J. Physiol.*, **482**(2), 275–281.

TSIEN, R.W., ELLINOR, P.T. & HORNE, W.A. (1991). Molecular diversity of voltage-dependent calcium channels. *Trends Pharmacol. Sci.*, **12**, 349–354.

WILLMER, E.N. (1970). *Cytology and Evolution.* 2nd edn. New York: Academic Press.

(Received February 27, 1995
Revised July 10, 1995
Accepted July 24, 1995)